Nonsingular Constant Modulus Equalizer for PDM-QPSK Coherent Optical Receivers

Athanasios Vgenis, Constantinos S. Petrou, Constantinos B. Papadias, *Senior Member, IEEE*, Ioannis Roudas, and Lambros Raptis

***Abstract*—Adaptive electronic equalizers using the constant modulus algorithm (CMA) algorithm often converge to a singular coefficient matrix that produces the same signal at multiple outputs. We address this issue in the context of optical communications systems with polarization-division multiplexing and coherent receivers. We study, by computer simulation, the performance of multiuser CMA equalizer, an enhanced CMA equalizer initially proposed for use in wireless multiuser and later multiple-input/multiple-output communications systems. We show that the proposed adaptive electronic equalizer does not exhibit singularities and, therefore, is superior to the commonly used CMA equalizer.**

***Index Terms*—Coherent detection, constant modulus algorithm (CMA), polarization-division multiplexing (PDM).**

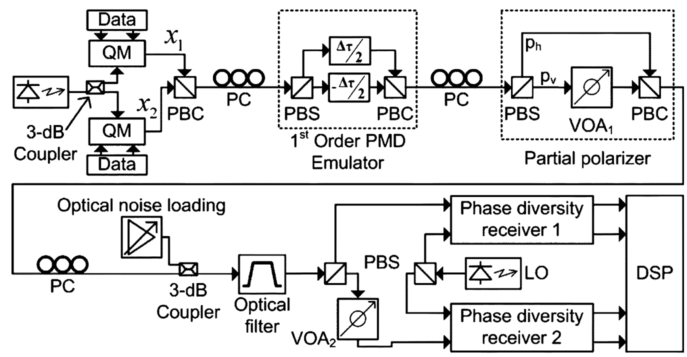

Fig. 1. Block diagram of the simulated system. (Symbols: QM: Quadrature modulator; x_1, x_2: Transmitted signals; $\Delta\tau$: Differential group delay; LO: Local oscillator).

I. Introduction

POLARIZATION- and phase-diversity coherent receivers, in combination with polarization-division multiplexing (PDM) and M-ary modulation formats, are a promising solution for high-capacity optical communications systems. M-ary modulation formats achieve high effective bit rates using lower symbol rates. PDM further doubles the spectral efficiency by assigning two independent signals to two orthogonal polarizations. Polarization- and phase-diversity coherent receivers enable electronic polarization demultiplexing, unlimited equalization of linear transmission impairments, and phase tracking [1]–[3]. Blind adaptive equalization is mostly performed, usually by employing a butterfly-structure multiple-input/multiple-output adaptive electronic equalizer using the constant modulus algorithm (CMA) [1]–[3]. The aforementioned equalizer employs a cost function that does not discriminate between the two equalized signals. Hence, it is common that this algorithm converges to a tap-weight setup that produces the same transmitted signal at both equalizer outputs, usually the one that arrived with higher power at the receiver [4]. The equalizer matrix in this case becomes singular. This problem can be circumvented by frequently monitoring the equalizer's matrix determinant and reinitializing the tap-weights when singularity is approached [2], a solution that is practical, but could cause discontinuity issues at the equalizer output. Alternatively, [5] proposes a special initialization procedure, which avoids singularity at start up, without overruling the possibility of such to occur subsequently. A computationally demanding equalization algorithm based on the independent component analysis method has also been proposed [6]. In [7], singularity is avoided by placing constraints on the equalizer coefficients, but use of only single-tap filters does not allow for compensation of transmission effects.

In this letter, we propose the use of multiuser CMA (MU-CMA) [4], which is an extension of the conventional CMA to the multiple input case, such that singularity is avoided. MU-CMA employs an enhanced cost function, penalizing the correlation between the two signals at the equalizer's outputs. We briefly describe the algorithm's principle of operation, and present simulation results, showing the algorithm's excellent performance against singularity. We also compare MU-CMA equalizer to the conventional CMA [1] equalizer.

II. System Description

The simulated optical coherent communication system is presented in Fig. 1. Two independent quadrature-phase-shift-keying (QPSK) signals x_1, x_2, at symbol rate R_S each, are generated and polarization-multiplexed using a polarization beam combiner (PBC). All PBCs and polarization beam splitters (PBSs) have aligned polarization axes. A first-order polarization-mode dispersion (PMD) emulator (PMD-1) and a partial polarizer play the role of the optical channel. Chromatic dispersion is neglected, since, usually, a dedicated

Manuscript received August 19, 2009; revised October 12, 2009. First published November 17, 2009; current version published December 16, 2009. This work was supported in part by the E.U.-European Social Fund (75%) and in part by the Greek Ministry of Development-GSRT (25%).

A. Vgenis, C. S. Petrou, and I. Roudas are with the Department of Electical and Computer Engineering, University of Patras, Rio 26500, Greece (e-mail: vgenis@ece.upatras.gr).

C. B. Papadias is with Athens Information Technology, Peania 19002, Greece (e-mail: papadias@ait.edu.gr).

L. Raptis resides in Athens, Greece (e-mail: lampros.raptis@gmail.com).

Color versions of one or more of the figures in this letter are available online at http://ieeexplore.ieee.org.

Digital Object Identifier 10.1109/LPT.2009.2035820

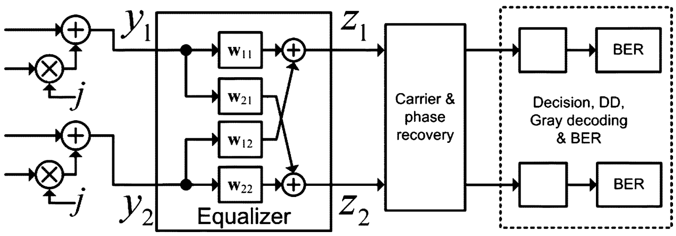

Fig. 2. Block diagram of the DSP section. Electronic lowpass filtering at 80% of the symbol rate, sampling at twice the symbol rate and ADC are not shown. (Symbols: y_1, y_2: Received signals; z_1, z_2: Equalized signals; DD: Differential decoding).

nonadaptive equalizer is used for its compensation [2]. At the partial polarizer, light is split into two orthogonal states of polarization (p_h, p_v) using a PBS. Before being recombined, polarization-dependent loss (PDL) is induced by attenuating the p_v-polarization signal component using a variable optical attenuator (VOA_1). Linear polarization controllers (PCs) at 45° and −45° are placed before and after PMD-1. Another PC is placed after the partial polarizer, with azimuth and ellipticity angles both equal to 30°. Optical noise loading and optical filtering with a 3-dB bandwidth of $5R_S$ follows. Within the coherent receiver, the signal that is fed into the second phase-diversity receiver is further attenuated using VOA_2. This way we model possible deviations from orthogonality at the eigenaxes of the receiver input PBS, mismatch between the responsivities of the two phase-diversity receivers' photodiodes, and differences between the respective analog/digital converters (ADCs), that could cause differential attenuation between the coherent receiver's branches.

The digital signal processing (DSP) unit of the receiver is shown in Fig. 2. Initially, the complex samples y_1, y_2 are generated and fed into the equalizer. Then, carrier and phase recovery is performed. Feedforward frequency [8] (FFFE) and phase (FFPE) [9] estimators are used. Finally, the samples are passed through a decision circuit, followed by a differential decoder and a Gray decoder. The recovered bit sequence is compared to the transmitted one and bit-error rate (BER) is measured by error counting.

III. MU-CMA Equalizer

We denote the samples at the two outputs of the equalizer for every symbol period k by $z_1[k],\ z_2[k]$, respectively, and the equalizer tap-weight matrix by $\mathbf{W} = [\mathbf{w}_{ij}],\ i,j = 1,2$, where $\mathbf{w}_{ij} = [w_{ij}^1 \dots w_{ij}^M]^T,\ i,j = 1,2$, are column vectors containing the values of the M tap-weights of each transversal filter of the equalizer. T denotes matrix transposition. The cost function of the MU-CMA equalizer, for normalized signals, is defined as [4]

$$J(\mathbf{W}) = E\left[\sum_{l=1}^{2}(|z_l|^2 - 1)^2\right] + 2\sum_{i=1}^{2}\sum_{\delta=\delta_1}^{\delta_2}|r_{ij}(\delta)|^2, \quad i + j = 3 \tag{1}$$

where the cross-correlation function between the equalizer outputs i, j is given by: $r_{ij}(\delta) = E[z_i[k]z_j^*[k-\delta]], \delta \in \mathbb{N}$. Star operator $(\cdot)^*$ denotes complex conjugation. Integers δ_1, δ_2 must be such, that both the minimum and the maximum possible time shifts between the two signals fall within the interval $[\delta_1, \delta_2]$. Time shifts between the two equalized signals are caused by PMD and differences in the lengths of optical and electrical connections. The first term of the cost function is the same as the conventional CMA equalizer [10], while the second term is an addition proposed in [4], which penalizes correlation between the equalizer's outputs.

A recursive equation for the update of the equalizer's tap-weights is derived using the stochastic gradient algorithm

$$\mathbf{W}(k+1) = \mathbf{W}(k) - \mu[\,\Delta_1(k) \quad \Delta_2(k)\,] \tag{2}$$

where μ is the algorithm's step-parameter and

$$\Delta_l(k) = 4(|z_l(k)|^2 - 1)z_l(k)\mathbf{Y}^*(k) + \sum_{\delta=0}^{\delta_2} r_{li}(\delta)z_i(k-\delta)\mathbf{Y}^*(k), \quad l = 1,2,\ l + i = 3. \tag{3}$$

In (3), $\mathbf{Y}[k] = [\mathbf{y}_1[k] \quad \mathbf{y}_2[k]]^T$, where $\mathbf{y}_1[k], \mathbf{y}_2[k]$ are line vectors containing the M fractionally spaced complex samples at each equalizer input.

IV. Results and Discussion

In this section, we compare the performance of CMA and MU-CMA equalizers for different values of differential group delay (DGD) of PMD-1 and the attenuation VOA_1 of the partial polarizer. For every pair of DGD-PDL values, we calculate, by Monte Carlo simulation, the optical signal-to-noise ratio (OSNR) penalty for $\mathrm{BER} = 10^{-3}$, with respect to the back-to-back case. The OSNR is measured in $1.25R_S$ resolution bandwidth. If the equalizer coefficient matrix becomes singular, one of the two transmitted signals is not produced at the outputs of the equalizer, and hence, the OSNR penalty becomes infinite. T_S denotes the symbol period.

In our simulations, the intermediate frequency offset between the local oscillator and the transmitter laser is set to $0.03R_S$ and the total laser linewidth is set to $10^{-4}R_S$ (equal to 300 and 1 MHz, respectively, for $R_S = 10$ GBd, that are representative experimental values [3]). The attenuation of the VOA_2 is set to 1 dB. The equalizers' parameters are $M = 20, \mu = 10^{-3}$, and $\delta_2 = 18$ for MU-CMA. Cross-correlation in (3) is calculated using time averaging over 20 symbols.

Initially, we study the occurrence of singularities in the use of the conventional CMA [1] equalizer. In Fig. 3, we show that the equalizer converges to a nonsingular matrix only for relatively small values of differential attenuation and DGD. For these cases, OSNR penalty is practically constant, about 0.2 dB. For DGD more than 0.45 T_S and PDL larger than 1 dB, singularity is always observed, for the system under study.

Next, we study the ability of the proposed MU-CMA equalizer to completely avoid convergence to singularities. Fig. 4 shows that the OSNR penalty for both x_1 and x_2 signals is never infinite. Since the partial polarizer affects the signal mean power and is placed prior to optical noise loading in our model, for low values of DGD it is expected that PDL will cause an increase in OSNR requirements for the attenuated tributary and a respective

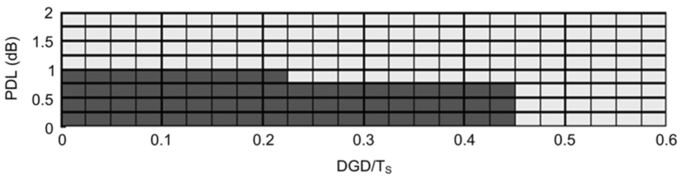

Fig. 3. Singularity map for the CMA equalizer. Dark color denotes normal operation and light color denotes singularity.

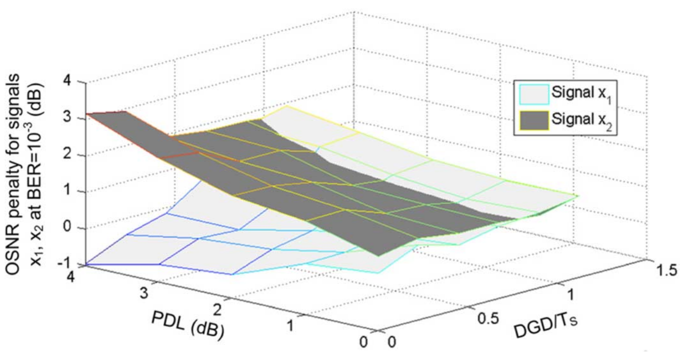

Fig. 4. MU-CMA equalizer: OSNR penalty for both signals at BER $= 10^{-3}$ versus DGD and PDL.

decrease in OSNR requirements for the nonattenuated tributary. Indeed, we show in Fig. 4 that the OSNR penalty for signal x_2 increases as PDL increases. OSNR penalty for signal x_1 decreases as the value of PDL increases, reaching even negative values when PDL takes high values. When both PDL and DGD take high values, OSNR penalties are similar for both signals. This is attributed to the strong power coupling between polarization tributaries caused by PMD, which roughly balances the difference in power caused by high values of PDL. A small increase in the OSNR penalty of about 0.3 dB relatively to the nonsingular cases studied for the CMA equalizer is observed. It is attributed to the increased gradient noise caused by the enhancement in the tap-weight update equation.

Finally, we study the convergence properties of the two equalizers by performing BER averaging over 100 computer runs. For the comparison of convergence speed, we impose a sudden increase of DGD from 0 to 0.4 T_S. PDL is equal to 0.5 dB and OSNR is equal to 11.5 dB. DGD and PDL values are chosen to have such values, so that no singularities are observed for the CMA equalizer, allowing for the two equalizers' performance to be compared. We separately optimize the equalizers' step-size parameter so that fastest convergence is achieved. In Fig. 5, we plot the evolution of the BER for the CMA and the MU-CMA equalizers. We see that both equalizers require about 400 symbol intervals for convergence. Next, we compare steady-state performance. We choose very small step-size parameters for the two equalizers and provide enough convergence time, so that steady-state BER is minimized. Steady-state BER is found to be equal to 4.4×10^{-4} for the MU-CMA equalizer and equal to 4.2×10^{-4}, for the CMA equalizer. This small difference is expected due to the increased gradient noise of the MU-CMA update equation.

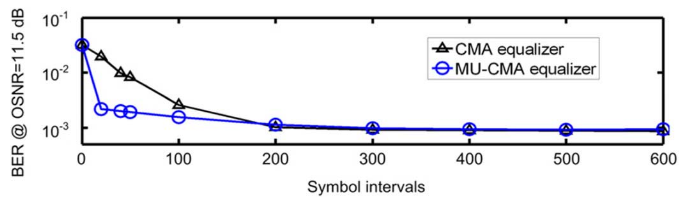

Fig. 5. BER time-evolution for the CMA and the MU-CMA equalizers.

V. CONCLUSION

In this letter, we studied the singularity problem of the CMA butterfly equalizer, commonly used with phase- and polarization-diversity coherent optical receivers. We proposed the use of multiuser CMA equalizer, a modified CMA equalizer that is capable of compensating for transmission impairments, such as PMD and PDL, completely avoiding convergence to a singular matrix. The MU-CMA equalizer's simplicity and capability of continuous operation are advantageous compared to other solutions proposed for solving the singularity issue. This equalizer guarantees, by design, convergence to a nonsingular matrix at all times. Tracking and steady-state performance is similar to that of the nonsingular operation of the conventional CMA.

REFERENCES

[1] J. Renaudier, G. Charlet, M. Salsi, O. B. Pardo, H. Mardoyan, P. Tran, and S. Bigo, "Linear fiber impairments mitigation of 40-Gbit/s polarization-multiplexed QPSK by digital processing in a coherent receiver," *J. Lightw. Technol.*, vol. 26, no. 1, pp. 36–42, Jan. 1, 2008.

[2] S. J. Savory, "Digital filters for coherent optical receivers," *Opt. Express*, vol. 16, no. 2, pp. 804–817, Jan. 2008.

[3] C. R. S. Fludger, T. Duthel, D. van den Borne, C. Schulien, E.-D. Schmidt, T. Wuth, J. Geyer, E. De Man, G. D. Khoe, and H. de Waardt, "Coherent equalization and POLMUX-RZ-DQPSK for robust 100-GE transmission," *J. Lightw. Technol.*, vol. 26, no. 1, pp. 64–72, Jan. 1, 2008.

[4] C. B. Papadias and A. J. Paulraj, "A constant modulus algorithm for multiuser signal separation in presence of delay spread using antenna arrays," *IEEE Signal Process. Lett.*, vol. 4, no. 6, pp. 178–181, Jun. 1997.

[5] L. Liu, Z. Tao, W. Yan, S. Oda, T. Hoshida, and J. C. Rasmussen, "Initial tap setup of constant modulus algorithm for polarization de-multiplexing in optical coherent receivers," in *Proc. OFC 2009*, San Diego, CA, Mar. 2009, Paper OMT2.

[6] H. Zhang, Z. Tao, L. Liu, S. Oda, T. Hoshida, and J. C. Rasmussen, "Polarization demultiplexing based on independent component analysis in optical coherent receivers," in *Proc. ECOC'08*, Brussels, Belgium, Sep. 2008, Paper Mo.3.D.5.

[7] K. Kikuchi, "Polarization-demultiplexing algorithm in the digital coherent receiver," in *Proc. IEEE LEOS Summer Topicals*, Acapulco, Mexico, Jul. 2008, Paper MC2.2.

[8] M. Morelli and U. Mengali, "Feedforward frequency estimation for PSK: A tutorial review," *Eur. Trans. Telecommun.*, vol. 9, no. 2, pp. 103–116, Mar./Apr. 1998.

[9] A. Viterbi, "Nonlinear estimation of PSK-modulated carrier phase with application to burst digital transmission," *IEEE Trans. Inf. Theory*, vol. IT-29, no. 4, pp. 543–551, Jul. 1983.

[10] D. Godard, "Self-recovering equalization and carrier tracking in two dimensional data communication systems," *IEEE Trans. Commun.*, vol. 28, no. 11, pp. 1867–1875, Nov. 1980.